Macromolecules
ARTICLE

Macromolecules **2009**, *42*, 8165–8171 **8165**
DOI: 10.1021/ma901413b

Surface Species of Titanium(IV) and Titanium(III) in $MgCl_2$-Supported Ziegler−Natta Catalysts. A Periodic Density Functional Theory Study

Denis V. Stukalov,* Igor L. Zilberberg, and Vladimir A. Zakharov

Boreskov Institute of Catalysis, Russian Academy of Sciences, Novosibirsk 630090, Russia

Received July 1, 2009; Revised Manuscript Received August 4, 2009

ABSTRACT: A systematic consideration of different Ti(IV) and Ti(III) species on the (104) and (110) $MgCl_2$ surfaces has been implemented within DFT using cyclic boundary conditions. Some new mononuclear and dinuclear surface complexes of Ti(IV) and Ti(III) were obtained due to implication of zip coordination mode. A possible spin state of dinuclear Ti(III) species was thoroughly studied: antiferromagnetic (ESR silent) state proved to be the most preferable in a number of cases. The zip antiferromagnetic Ti_2Cl_6 complexes residing on the dominant (104) $MgCl_2$ surface make it possible to rationalize the fact that the most part of Ti(III) incorporated in activated $MgCl_2$ is ESR silent. Besides, these species produce aspecific active sites, thus explaining that aspecific centers significantly prevail over stereospecific one according to kinetic data on the simplest $TiCl_4/MgCl_2 + AlR_3$ system.

1. Introduction

Polymerization over $MgCl_2$-supported Ziegler−Natta (ZN) catalysts is the most important method for industrial production of isotactic polypropylene.[1,2] The preparation procedure of these catalysts contains several steps which result in formation of active $MgCl_2$ and incorporation of $TiCl_4$ and a Lewis base (an "internal" donor) with formation of catalyst precursor. Finally, to generate active sites on the $MgCl_2$ surface, the precatalyst is activated by addition of trialkylaluminum ($AlEt_3$) mixed with a second Lewis base (an "external" donor).

A number of theoretical contributions have been performed to study both the $TiCl_4$ surface species formed at the precatalyst preparation stage and active sites originating from the former.[3−12] In order to model Ti surface species two $MgCl_2$ planes were generally considered since the activated $MgCl_2$ surface supposedly contains two types of the adsorption sites: the five-coordinated Mg cations residing on the (104) $MgCl_2$ surface and four-coordinated Mg cations residing on the (110) $MgCl_2$ surface.[13−17] A wide variety of the $TiCl_4$ species on these surfaces were proposed,[3,12] but that which have no Cl vacancies at the Ti atom are of the most interest since Raman spectroscopy shows that stable Ti complexes in the $TiCl_4/MgCl_2$ system include bound $TiCl_4$ molecules with Ti atoms in octahedral surroundings.[18] There are known to be two stable $TiCl_4$ surface complexes corresponding to this condition: mononuclear complex on the (110) $MgCl_2$ surface and dinuclear complex on the (104) $MgCl_2$ surface.[3] It is reasonable that both the complexes may simultaneously exist on the activated $MgCl_2$ surface since they are located on the different $MgCl_2$ planes, but the dinuclear Ti_2Cl_8 species are even the more preferable choice due to some arguments arising from the extended X-ray adsorption fine structure analysis.[19]

Interaction of the $TiCl_4/MgCl_2$ system with trialkylaluminum is known to result in creation of the Ti(III) and Ti(II) species as well as alkylation of these species with the formation of Ti−C bonds. Due to the presence of unpaired electron the Ti(III) species are an appropriate object for electron spin resonance (ESR) detection, nevertheless only 10−20% of Ti(III) give the ESR signal, and so the majority of Ti(III) was suggested to form polynuclear Ti species with low spin (LS) structure.[20−23] The known DFT calculations—conversely—indicate that dimerization of Ti^{4+} and Ti^{3+} species on the $MgCl_2$ surface is unfavorable by energy, and only on the (110) $MgCl_2$ surface dimeric Ti_2Cl_6 complexes have low spin (LS) structure, while on the (104) $MgCl_2$ surface the high spin (HS) structure is predicted.[3,12] In this connection, some questions arise. What is the motive force of Ti agglomeration on the support surface? Is the main part of Ti^{3+} localized only on the (110) $MgCl_2$ surface?

Very recently, based on periodic DFT calculations, Busico et al. concluded that the five-coordinated Mg cations are the dominant adsorption sites since the surface energy of (104) is lower than that of (110).[17] Later this conclusion was confirmed by DRIFT study of carbonyl compound adsorption on the $MgCl_2$ samples activated in the different ways.[24] It was clearly demonstrated that the (104) surface significantly prevails over the (110) $MgCl_2$ surface in both cases: chemically activated and dry-milled $MgCl_2$.[24] Moreover, it is these types of $MgCl_2$ that are used for ESR investigation in refs 20 and 21. Finally, all these observations have caused us to revise the concepts of Ti state on the $MgCl_2$ surface because the Ti surface species proposed in the literature make it impossible to explain some ESR and kinetic data on the resulting catalytic system ($TiCl_4/MgCl_2$ interacted with trialkylaluminum) if the adsorption site distribution appointed is taken into account. As for the ESR data, since known DFT calculations reveal ESR silent Ti(III) species only on the (110) $MgCl_2$ surface, it is necessary to be of opinion that $TiCl_4$ is predominantly adsorbed on the (110) $MgCl_2$ surface, but it is in contradiction with the fact that the dominant adsorption sites are the five-coordinated Mg cations residing on the (104) $MgCl_2$ surface.[17,24] The same problem emerges upon analysis of the kinetic data and polymer structure. According to the data on the number of active centers in the simplest catalyst $TiCl_4/MgCl_2 + AlEt_3$ aspecific sites significantly prevail over stereospecific sites.[25] In turn, it is largely believed that the (104) $MgCl_2$ surface contains mainly stereospecific sites because both the Ti_2Cl_7 and Ti_2Cl_6 species forming at the reduction of the Ti_2Cl_8 species are

*To whom correspondence should be addressed. E-mail: stukalov@catalysis.ru. Fax: +7 383 330 96 87.

Published on Web 08/18/2009

stereospecific centers.[11,12,26] The (110) $MgCl_2$ surface has been long believed to be nonstereospesific since it seemed only mononuclear Ti species existed on that,[26] but recently Terano et al. have suggested a new dinuclear Ti_2Cl_8 complex on the (110) $MgCl_2$ surface which may be a precursor of stereospecific active centers, casting a shadow on the monopoly of the (104) $MgCl_2$ surface being stereospecific.[12] Nevertheless, based on the known theoretical calculations, it is impossible to explain the fact that the most aspecific active sites must be situated on the (104) $MgCl_2$ surface owing to the fact that this surface contains the majority of the potential adsorption sites.[17,24]

To rationalize these facts an attention in the present paper is focused to modeling the dinuclear Ti species on the (104) and (110) $MgCl_2$ surfaces and studying their electronic structure using periodic DFT calculations. A number of new Ti species were obtained due to using zip coordination mode on both the surfaces. New dimeric Ti_2Cl_8 species revealed on the (104) $MgCl_2$ surface make it possible to explain the experimental data mentioned above since upon reduction by trialkylaluminum these complexes can produce both isospecific (ESR active) and aspecific (ESR silent) active sites.

2. Computational Details

The $MgCl_2$ bulk was assumed to be in the α crystalline phase with the lattice constants 3.64 and 17.67 Å.[27] The (104) and (110) $MgCl_2$ surfaces were expressed as repeated slabs with 2 and 3 atomic layers, accordingly. The periodically repeated slabs were separated one from another by a vacuum region of about 12 Å. The following surface unit cells were used: (4 × 2) having 16 $MgCl_2$ for modeling of Ti complexes located on the (104) surface; (2 × 2) having 12 $MgCl_2$ for modeling of Ti complexes located on the (110) surface. During the geometry optimization one bottom layer of atoms was fixed in the positions of the ideal crystal.

The calculations of the periodic models were carried out within DFT with exchange-correlation Perdew−Wang functional (PW91).[28] The plane wave basis set was limited by a 20 Ry energy cutoff. Atomic cores were described by ultrasoft pseudopotentials.[29] A 2 × 2 × 1 Monkhorst−Pack grid was applied. A convergence criterion was 10^{-6} hartree for SCF calculations, 10^{-4} Hartree for geometry optimization and 10^{-3} hartree/bohr for the maximum force. Closed-shell DFT was used for the calculation of the surface $TiCl_4$ and Ti_2Cl_8 species, whereas spin-polarized DFT was employed for the calculation of the surface species with Ti(III). The Lowdin analysis was used for determination of atomic spin densities. The calculations were performed using PWSCF package.[30]

Adsorption energies are computed as $E_{ads} = -E_\Sigma + E_1 + E_2$, where E_Σ, E_1 and E_2 are the total energies of the adsorption species, isolated $TiCl_4$ or $TiCl_3$ and unit cell of the relaxed surface, respectively. Since E_1, E_2 and $E_\Sigma < 0$, adsorption energy $E_{ads} > 0$ if adsorbate is bound with the surface. Relative adsorption energies for dinuclear Ti species are computed as $E_{relative} = E_{ads}$(dinuclear species)/2 − E_{ads}(mononuclear Ti species).

3. Results and Discussion

Very recently, Busico et al. concluded that the dominant lateral $MgCl_2$ surface was the plane which contains only the five-coordinated Mg cations and which is indexed as (104) rather than (100).[17] The structures of the (104) and (100) surfaces for α-$MgCl_2$ are presented in Figure 1. Since the (100) $MgCl_2$ surface contains three-, five- and six-coordinated Mg cations and has a jagged edge, zip coordination mode is unrealizable on such surface and therefore known theoretical studies considered $TiCl_4$ complexes located within one Cl−Mg−Cl layer. In turn, the structure of the (104) $MgCl_2$ surface enable to generate a new dinuclear Ti complex, which is located within two Cl−Mg−Cl layers, and so it can be referred to as zip Ti_2Cl_8 complex.

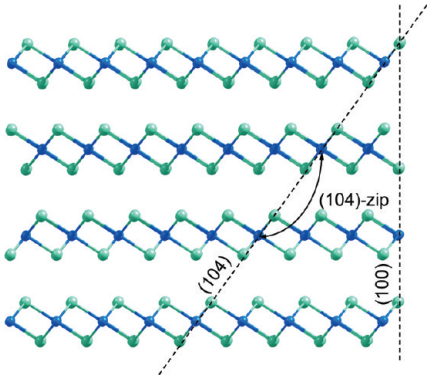

Figure 1. Structures of the (104) and (100) $MgCl_2$ surfaces. Mg atoms are colored in dark blue; Cl atoms are colored in sage-green. The double arrow curve represents the (104)-zip coordination mode.

Thus, there can be three types of Ti(IV) species on the (104) $MgCl_2$ surface: mononuclear and dinuclear species residing on a Cl−Mg−Cl layer and dinuclear species residing on two Cl−Mg−Cl layers. The optimized structures of these complexes are presented in Figure 2. The adsorption energies were 8.4, 32.3, and 35.0 kcal/mol for complexes **1a**−**1c**, respectively (see Table 1). Mononuclear **1a** and dinuclear **1b** structures were considered in literature more than once,[3,6,12] so it is worth comparing the adsorption energy magnitude obtained with previous ones to give an impression of the sensitivity of the results to the choice of calculation method. The adsorption energy of mononuclear complex **1a** proved to be slightly bigger than in works of Cavallo et al. (5.0 kcal/mol)[3] and Ziegler et al.(7.3 kcal/mol)[6] and somewhat smaller than in work of Terano et al. (11.7 kcal/mol).[12] On the whole, the present results are similar to the previous ones, with some differences being likely to relate to choice of DFT functional or geometric model (first of all, the slab thickness). Since far greater slab thickness was employed in work of Terano et al.,[12] and even the increased adsorption energy was obtained, in the present work overestimation of adsorption energy in comparison with works of Cavallo et al.[3] and Ziegler et al.[6] is due to DFT functional choice rather than to a small number of $MgCl_2$ layers in the slab. The significance of DFT functional choice becomes more apparent from the great discrepancy which was observed in case of Corradini dimers **1b**: the corresponding adsorption energy was much more than in literature.[3,12] Actually, the latter fact cannot be related to geometric model choice (in particular, slab thickness) since the adsorption energy of mononuclear Ti species is in range of literature data.

$TiCl_4$ is known to form strong complexes on the $MgCl_2$ surface.[1,2,18] If this is the case, not only must Ti surface species exhibit a positive adsorption energy but also this binding energy must be large enough to overcome an entropic barrier due to the loss of translational and rotational degrees of freedom.[6] The estimation of entropic barrier gives a value of 13.0 kcal/mol at 350 K.[6] No $TiCl_4$ complexes on the (104) $MgCl_2$ surface considered in literature so far exhibit adsorption energy larger than this magnitude.[3,6,12] Thus, this is the first theoretical work that demonstrates the possibility for rationalization of $TiCl_4$ forming strong complexes on the (104) $MgCl_2$ surface: adsorption energy for species **1b** is 16.1 kcal/mol Ti atoms.

Besides, the large energy gain of dinuclear species **1b** and **1c** as regard to mononuclear one **1a** (8−9 kcal/mol) enables to explain the ESR data which clearly point to formation of Ti agglomerates on the $MgCl_2$ surface.[20−23] Actually, it is unlikely for Ti species to migrate on the $MgCl_2$ surface during reduction stage since according experimental evidence even unreduced $TiCl_4$ surface complexes are strongly bound to the $MgCl_2$ surface.[1,2,18] The **1c**

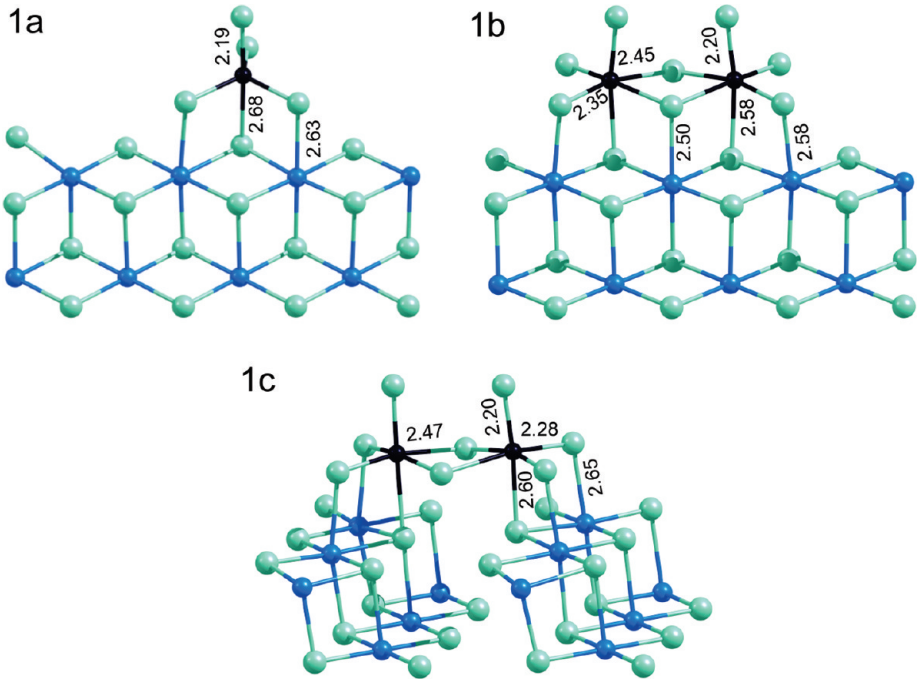

Figure 2. Complexes of Ti(IV) on the (104) $MgCl_2$ surface. Ti, Mg, and Cl atoms are colored in black, dark blue, and sage-green, respectively.

Table 1. Adsorption Energies, Ti−Ti Distances, and Spin States of Ti(IV) and Ti(III) Species on the (104) $MgCl_2$ Surface

						spin magnetic moment[c]	
label	species	E_{ads}, kcal/mol	$E_{relative}$[a], v	Ti−Ti distance, Å	Δn[b]	Ti(1)[d]	Ti(2)[d]
1a	$TiCl_4$	8.4	0		0		
1b	Ti_2Cl_8	32.3	+7.8	3.89	0		
1c	Ti_2Cl_8	35.0	+9.1	3.75	0		
2a	$TiCl_3$	28.2	0		1	+1.03	
2b	Ti_2Cl_6	85.9	+14.8	2.95	0	0.00	0.00
2c	Ti_2Cl_6	80.9	+12.3	3.60	2	+1.04	+1.04
2d	Ti_2Cl_6	84.0	+13.8	3.85	2	+1.04	+1.04
2e	Ti_2Cl_6	87.0	+15.3	3.35	0	0.00	0.00
2f	Ti_2Cl_6	95.0	+19.3	3.52	0	+1.09	−1.09
2g	Ti_2Cl_6	85.6	+14.6	3.45	2	+1.03	+1.03
3a	Ti_2Cl_6Et	56.7[e]	0	4.44	1	+0.64	+0.50
3b	Ti_2Cl_6Et	63.2[e]	+6.5	3.62	1	+0.57	+0.51
3c	Ti_2Cl_5Et	62.4[e]	0	4.16	0	+0.91	−0.86
3d	Ti_2Cl_5Et	69.7[e]	+7.3	3.42	0	+0.97	−0.93

[a] $E_{relative} = E_{ads}$(dimeric species)/2 − E_{ads}(monomeric species), $E_{relative}$(monomeric species) = 0. [b] $\Delta n = n$(spin-up) − n(spin-down). [c] In bohr magnetons. [d] In corresponding figures, Ti(1) is the left Ti atom, whereas Ti(2) is the right Ti atom. [e] Adsorption energy with respect to separated $TiCl_2Et$ and $TiCl_4$ (for **3a** and **3b**) or $TiCl_3$ (for **3c** and **3d**) species.

species were slightly (2.7 kcal/mol) more favor as compared to **1b** species. The highest stability of dinuclear **1c** structure is obviously caused by the formation of two bridge bonds between the Ti atoms (which are absent in **1a** species) and coordination with four surface Mg cations (whereas **1b** structure is coordinated only with three surface Mg cations). Therefore, new dinuclear **1c** complex may be a main precursor of active centers in the catalyst because of its highest relative stability and location on the dominant (104) $MgCl_2$ surface.

Approaching the active centers, the species **1a**−**1c** were reduced to mononuclear $TiCl_3$ and dinuclear Ti_2Cl_6 species by removing one or two Cl atoms, accordingly. The structures and stabilities for these complexes are given in Figure 3 and Table 1. The reduced species had a stronger tendency to dimerization than the Ti(IV) species obviously due to the interaction between spins localized on the Ti(III) atoms. Since the Ti_2Cl_6 species have potentially two unpaired electrons, several spin states for each complex are possible. The closed-shell singlet (LS) and triplet (HS) states were found for the Ti_2Cl_6 species located within one Cl−Mg−Cl layer (Figure 3). The LS structure **2b** (that is the structure in which there are no any unpaired spins) was 1.9 kcal/mol more favor than the HS structure **2d** (that is the structure with two unpaired spins), thus indicating that Ti_2Cl_6 species located within one Cl−Mg−Cl layer are likely ESR silent. Besides, starting from the different initial geometries two conformations were found for the HS structure (**2c** and **2d**). The structure **2d** with terminal Cl atoms located closer to the (104) $MgCl_2$ surface was more stable than the structure **2c** probable due to the electrostatic interaction between the Cl anions of Ti_2Cl_6 and $MgCl_2$ surface. As for catalytic properties of dimeric Ti species residing within one Cl−Mg−Cl layer on the (104) $MgCl_2$ surface, the most stable structure **2b** must generate stereospecific active centers, similar to Ti_2Cl_7 complex forming upon reduction only one of two Ti atoms in structure **1b**, due to the steric effect of the Cl(Ti) atom that is the most distant from the surface.

For zip Ti_2Cl_6 species, three spin states were obtained: closed-shell singlet (LS state), triplet (HS state), and, in contrast to Ti_2Cl_6 species located within a Cl−Mg−Cl layer, broken

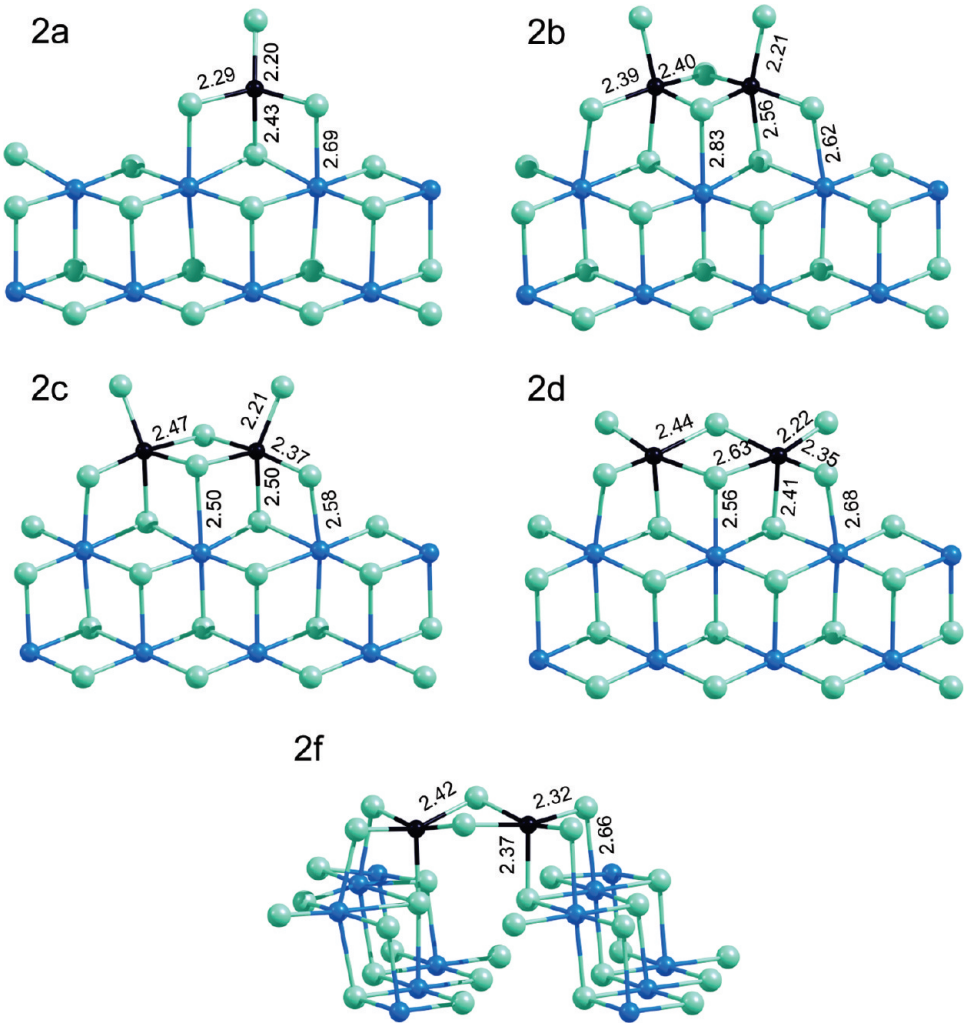

Figure 3. Complexes of Ti(III) on the (104) $MgCl_2$ surface. Ti, Mg, and Cl atoms are colored in black, dark blue, and sage-green, respectively.

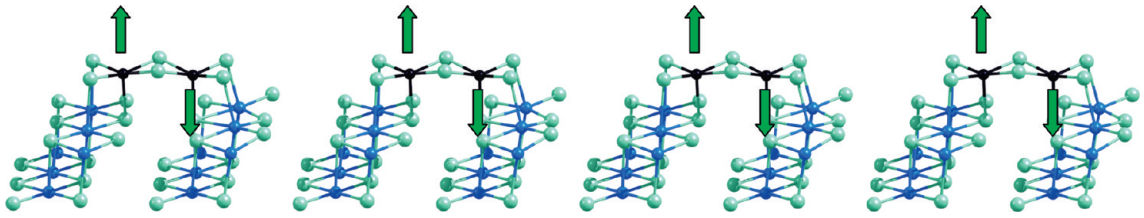

Figure 4. Spin wave generated by antiferromagnetic zip Ti_2Cl_6 complexes (**2f**) on the (104) $MgCl_2$ surface. The arrows show spin magnetic moment on the Ti atoms.

symmetry singlet (antiferromagnetic), in which the first Ti atom has positive spin magnetic moment while the second Ti atom has negative spin magnetic moment (Figure 4 demonstrates the resulting spin wave on the (104) $MgCl_2$ surface), although the total spin magnetic moment is 0 as in case of closed-shell singlet. All these states had geometries quite similar to each other and so only the more stable **2f** structure is given in Figure 3. It is quite unexpected that in the case of the zip Ti_2Cl_6 complex the antiferromagnetic **2f** state is significantly more stable (by 8−9 kcal/mol) as compared to closed-shell singlet **2e** and triplet **2g** states, whereas in the case of the Ti_2Cl_6 complex located within a Cl−Mg−Cl layer we failed to succeed in producing an antiferromagnetic state at all. Moreover, structure **2f** is the most stable among all the calculated $TiCl_3$ and Ti_2Cl_6 species (see Table 1). Since spins localized on the Ti atoms are bound in antiferromagnetic **2f** state, zip Ti_2Cl_6 species residing on the dominant (104) $MgCl_2$ surface should be expected to be ESR silent. It therefore allows us to rationalize the fact that the most Ti(III) incorporated in activated $MgCl_2$ is ESR silent. Thus, zip Ti species **2f** are the most probable Ti(III) state in the $TiCl_4/MgCl_2$ sample interacted with trialkylaluminum, and so further we will consider the stereoregulating properties of active centers which can be generated upon the reduction of zip Ti_2Cl_8 species **1c**.

Interaction of zip Ti_2Cl_8 species with triethylaluminum can result in the elimination of several Cl atoms and formation of Ti−C bonds. To take into account the simplest active centers of Ti(III) one or two Cl atoms were removed, and one Cl atom was substituted by ethyl radical. The corresponding structures are presented in Figure 5. The structures with two bridge Cl atoms **3b** and **3d** were more stable than the structures with one bridge Cl atom **3a** and **3c** (Table 1). The ESR active structure **3b** can be supposed to behave as a stereospecific center

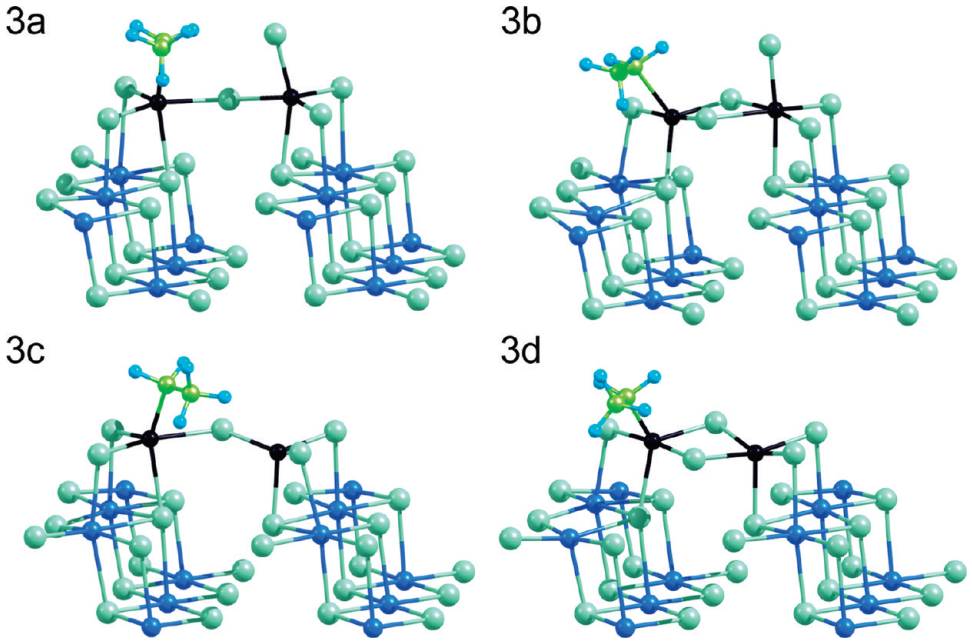

Figure 5. Active centers generated from zip Ti_2Cl_8 species (**1c**) on the (104) $MgCl_2$ surface. Mg and Cl atoms are represented by the bigger balls colored in dark blue and sage-green, accordingly. Ti, C, and H atoms are depicted by the smaller balls colored in black, green, and azure, respectively.

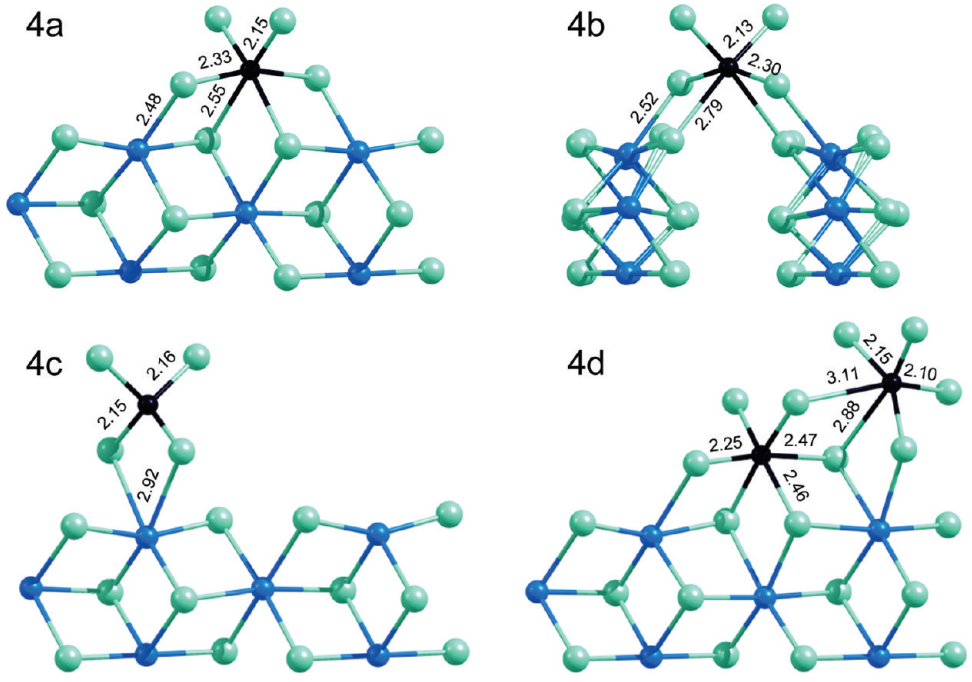

Figure 6. Complexes of Ti(IV) on the (110) $MgCl_2$ surface. Ti, Mg, and Cl atoms are colored in black, dark blue, and sage-green, respectively.

(which produces isotactic polypropylene) due to the strong steric effect from the terminal Cl atom on the alkyl radical (growing polymer chain), while the ESR silent structure **3d** is an aspecific center (which produces atactic polypropylene) since the terminal Cl atom is absent.

It should be noted that dinuclear Ti(IV) species **1b** located within one Cl−Mg−Cl layer on the (104) $MgCl_2$ surface, which are considered so far, can only result in the formation of stereospecific centers upon the reduction to Ti(III). Therefore, such complexes can not explain the fact that in the absence of Lewis bases aspecific sites dominate over stereospecific sites.[25] In turn, zip Ti_2Cl_8 species also residing on the dominant (104) $MgCl_2$ surface upon the reduction can produce both aspecific Ti_2Cl_5Et and stereospecific Ti_2Cl_6Et sites. The former must prevail over the latter because the amount of Ti(IV), which makes up the Ti_2Cl_6Et sites, is small enough in catalyst. Thus, zip Ti_2Cl_6 complexes make it possible to rationalize the domination of aspecific active sites over stereospecific one and the absence of ESR signal for the most Ti(III) on the activated $MgCl_2$ surface.

The (110) $MgCl_2$ surface, which can be supposed to contain less potential adsorption sites than the (104) $MgCl_2$ surface, may be one of the main source of active center heterogeneity, and so it deserves careful consideration too. In contrast to the (104) surface there is a wide variety of mononuclear Ti(IV) species on the (110) surface: octahedral complex located within a Cl−Mg−Cl layer **4a**, octahedral complex located within two Cl−Mg−Cl layers **4b** and

tetrahedral complex **4c** (Figure 6). The octahedral species **4a** are more stable by about twice times (Table 2) than the others because Ti atom in that has the highest possible number of neighboring Cl atoms and geometry of corresponding adsorption site enables to form the Ti−Cl($MgCl_2$) bonds with length close to that of the Mg($MgCl_2$)−Cl($TiCl_4$).

Recently an idea of dimeric Ti species on the (110) surface has been suggested by Terano et al.[12] To build a complete picture we following Terano modeled dimeric Ti_2Cl_8 complex too. It is unexpected that the dimeric species **4d** have the same stability as the monomeric species **4a**, though one Ti atom in **4d** has a single Cl($TiCl_4$)−Mg bond (Figure 6). The opposite result—an extremely low stability of dimeric Ti_2Cl_8 species on the (110) surface as compared to mononuclear one—was obtained in ref 12.

Table 2. Adsorption Energies, Ti−Ti Distances, and Spin States of Ti(IV) and Ti(III) Species on the (110) $MgCl_2$ Surface

						spin magnetic moment[c]	
label	species	E_{ads}, kcal/mol	$E_{relative}$[a], kcal/mol Ti	Ti−Ti distance, Å	Δn[b]	Ti(1)[d]	Ti(2)[d]
4a	$TiCl_4$	22.8	0		0		
4b	$TiCl_4$	10.1	−12.7		0		
4c	$TiCl_4$	12.3	−10.5		0		
4d	Ti_2Cl_8	46.8	+0.6	4.12	0		
5a	$TiCl_3$	41.3	0		1	+1.01	
5b	Ti_2Cl_6	107.0	+12.2	2.95	0	0.00	0.00
5c	Ti_2Cl_6	111.3	+14.4	3.23	0	+1.04	−1.00
5d	Ti_2Cl_6	108.2	+12.8	3.34	2	+0.74	+1.32
5e	Ti_2Cl_6	99.5	+8.4	3.61	0	0.00	0.00
5f	Ti_2Cl_6	107.4	+12.4	3.66	0	+0.84	−0.89
5g	Ti_2Cl_6	105.6	+11.5	3.63	2	+1.50	+0.53

[a] $E_{relative} = E_{ads}$(dimeric species)/2 − E_{ads}(monomeric species), $E_{relative}$(monomeric species) = 0. [b] $\Delta n = n$(spin-up) − n(spin-down). [c] In bohr magnetons. [d] In the corresponding figures, Ti(1) is the left Ti atom, whereas Ti(2) is the right Ti atom.

This difference can be associated with the fact that PBE functional was used in that work,[12] whereas PW91 functional was employed in the present contribution. A surprisingly large and consistent discrepancy between PBE and PW91 results was observed for example in ref 31. Thus, the mononuclear **4a** and dinuclear **4d** species can be believed to the most plausible Ti(IV) state on the (110) $MgCl_2$ surface. An additional argument in favor of **4d** species formation is more molar ration Ti/Mg = 4/3 as compared to equimolar one for **4a** species that may provide a larger energy gain for all the (110) $MgCl_2$ surface.

To analyze ESR sensitivity of the (110) $MgCl_2$ surface **4a** and **4d** complexes as the most reliable were reduced by removing one or two Cl atoms in order to produce monomeric $TiCl_3$ and dimeric Ti_2Cl_6 species, accordingly (see Figure 7). Since complex **4d** has two groups of nonequivalent dangling Cl atoms, two isomers are potential: **5c** species with two dangling Cl atoms removed from the right Ti atom and **5f** species with ones removed from the right and left Ti atoms. For each of these dimeric species three spin states were considered: closed-shell singlet, triplet and broken symmetry singlet. The antiferromagnetic state (broken symmetry singlet) was the most preferable among them for both these species: energy profit with regard to triplet state was 3.1 kcal/mol for the former species and 1.8 kcal/mol for the latter species. As a result, both the complexes can be supposed to be ESR silent.

Although **5c** species are 4.9 kcal/mol more stable than **5f**, we believe that both the complexes are possible because the mechanism of $TiCl_4$ species reduction by trialkylaluminum should be expected to determine largely the preference of one species or another to form rather than relative stability of the resulting complexes. As pointed out in ref 12, the species **5c** seems to generate stereoselective active sites due to the steric effect of the terminal Cl atom at the right Ti atom, however the rigorous evidence of this assumption is still pending. The **5a** and **5f** species would certainly produce aspecific active centers as they possess no chirality. Thus, with equal facility several Ti(III) complexes on the (110) surface are possible: ESR active aspecific species **5a**,

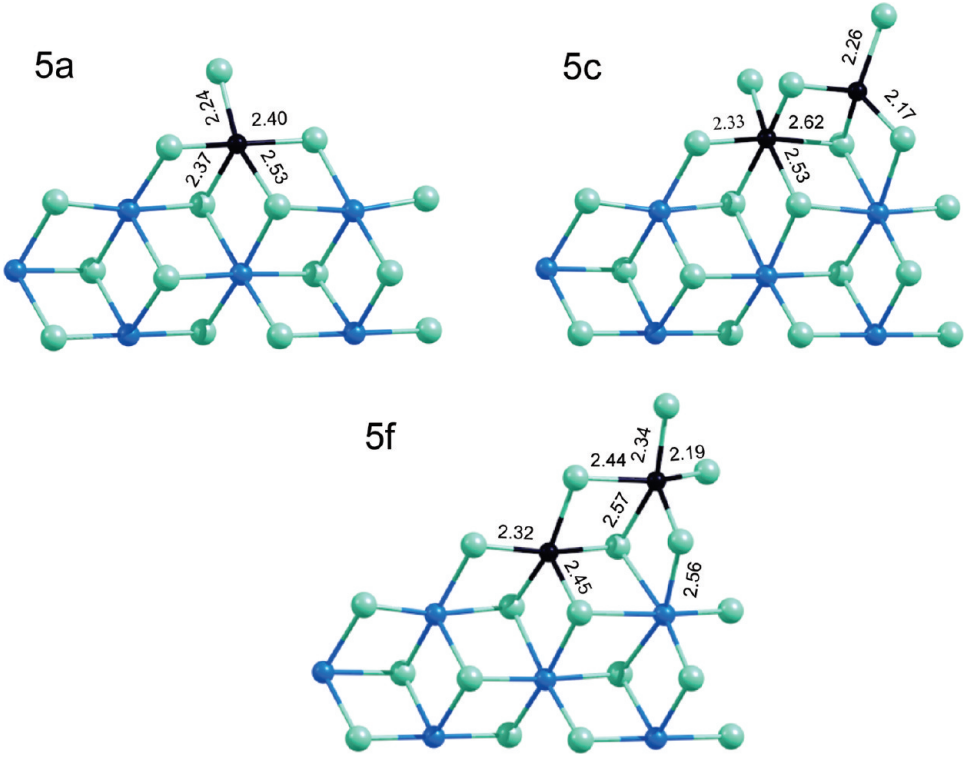

Figure 7. Complexes of Ti(III) on the (110) $MgCl_2$ surface. Ti, Mg, and Cl atoms are colored in black, dark blue, and sage-green, respectively.

ESR silent aspecific species **5f** and ESR silent stereospecific species **5c**. Taking into account experimental fact that 10−20% of Ti(III) are ESR active in the $TiCl_4/MgCl_2 + AlR_3$ system, one may conclude that this part of Ti is likely to associate mainly with the mononuclear Ti species **5a** on the (110) $MgCl_2$ surface because on the (104) $MgCl_2$ surface the dinuclear Ti_2Cl_8 complexes producing ESR silent Ti(III) species are significantly more favorable as compared to the mononuclear $TiCl_4$ species giving ESR active Ti(III) species.

4. Conclusions

A systematic consideration of different Ti(IV) and Ti(III) species on the (104) and (110) $MgCl_2$ surfaces have been implemented within DFT using cyclic boundary conditions. Taking into consideration zip coordination mode on both the surfaces a number of new Ti complexes were obtained: mononuclear zip Ti species on the (110) surface and dinuclear zip Ti complexes on the (104) surface. The latter are of a great interest since: (i) zip Ti_2Cl_8 complex proved to be the most stable among all Ti(IV) species residing on the (104) $MgCl_2$ surface; (ii) reduction of such species produces antiferromagnetic (ESR silent) Ti_2Cl_6 structure which is also the most favored among all the other Ti(III) species on this surface; (iii) zip Ti_2Cl_8 species can produce both aspecific (ESR silent) and stereospecific (ESR active) centers in contrast to Ti_2Cl_8 species located within one Cl−Mg−Cl layer on the (104) surface that must generate only stereospecific centers. Since dinuclear zip complexes of Ti(IV) and Ti(III) are located on the dominant (104) $MgCl_2$ surface, it allows us to rationalize the following experimental facts: (i) in the simplest $TiCl_4/MgCl_2 + AlR_3$ system aspecific sites significantly prevail over stereospecific sites; (ii) the most amount of Ti(III) incorporated in activated $MgCl_2$ is ESR silent because antiferromagnetic interaction takes place in zip Ti_2Cl_6 species. The remaining 10−20% of Ti(III) species, being ESR active, are likely to associate mainly with mononuclear Ti species on the (110) $MgCl_2$ surface since mononuclear Ti(IV) species are as stable as dinuclear one on the (110) surface, whereas on the (104) $MgCl_2$ surface mononuclear $TiCl_4$ species producing ESR active Ti(III) species are significantly less favorable as compared to dinuclear Ti_2Cl_8 complexes giving ESR silent Ti(III) species.

Although the analysis involved is certainly not ultimate and dogmatic, we believe that it will promote a deeper insight into the multiplicity and structure of the real active sites in $MgCl_2$-supported Ziegler−Natta catalysts.

Acknowledgment. The authors are grateful to Sergey Malykhin and Alexander Shubin (Boreskov Institute of Catalysis) for technical support.

References and Notes

(1) Barbe, P. C.; Ceccin, G.; Noristi, L. *Adv. Polym. Sci.* **1987**, *81*, 1.
(2) Albizzati, E.; Giannini, U.; Collina, G.; Noristi, L.; Resconi, L. Catalysts and Polymerizations. In *Polypropylene Handbook*; Moore, E. P., Jr., Ed.; Hanser-Gardner Publications: Cincinnati, OH, 1996; Chapter 2.
(3) Monaco, G.; Toto, M.; Guerra, G.; Corradini, P.; Cavallo, L. *Macromolecules* **2000**, *33*, 8953.
(4) Boero, M.; Parrinello, M.; Weiss, H.; Huffer, S. *J. Phys. Chem. A* **2001**, *105*, 5096.
(5) Martinsky, C.; Minot, C.; Ricart, J. M. *Surf. Sci.* **2001**, *490*, 237.
(6) Seth, M.; Margl, P. M.; Ziegler, T. *Macromolecules* **2002**, *35*, 7815.
(7) Seth, M.; Ziegler, T. *Macromolecules* **2003**, *36*, 6613.
(8) Seth, M.; Ziegler, T. *Macromolecules* **2004**, *37*, 9191.
(9) Taniike, T.; Terano, M. *Macromol. Rapid Commun.* **2007**, *28*, 1918.
(10) Correa, A.; Piemontesi, F.; Morini, G.; Cavallo, L. *Macromolecules* **2007**, *40*, 9181.
(11) Lee, J. W.; Jo, W. H. *J. Organomet. Chem.* **2007**, *692*, 4639.
(12) Taniike, T.; Terano, M. *Macromol. Rapid Commun.* **2008**, *29*, 1472.
(13) Giannini, U. *Makromol. Chem Suppl.* **1981**, *5*, 216.
(14) Kim, S. H.; Tewell, C. R.; Somorjai, G. A. *Langmuir* **2000**, *16*, 9414.
(15) Trubitsyn, D. A.; Zakharov, V. A.; Zakharov, I. I. *J. Mol. Catal. A: Chem.* **2007**, *270*, 164.
(16) Andoni, A.; Chadwick, J. C.; Niemantsverdriet, J. W.; Thune, P. *J. Catal.* **2008**, *257*, 81.
(17) Busico, V.; Causa, M.; Cipullo, R.; Credendino, R.; Cutillo, F.; Friederichs, N.; Lamanna, R.; Segre, A.; Castelli, V. *J. Phys. Chem. C* **2008**, *112*, 1081.
(18) Brambilla, L.; Zerbi, G.; Piemontesi, F.; Nascetti, S.; Morini, G. *J. Mol. Catal. A: Chem.* **2007**, *263*, 103.
(19) Potapov, A. G.; Kriventsov, V. V.; Kochubey, D. I.; Bukatov, G. D.; Zakharov, V. A. *Macromol. Chem. Phys.* **1997**, *198*, 3477.
(20) Zakharov, V. A.; Makhtarulin, S. I.; Poluboyarov, V. A.; Anufrienko, V. F. *Makromol. Chem.* **1984**, *185*, 1781.
(21) Sergeev, S. A.; Poluboyarov, V. A.; Zakharov, V. A.; Anufrienko, V. F.; Bukatov, G. D. *Makromol. Chem.* **1985**, *186*, 243.
(22) Brant, P.; Speca, A. *Macromolecules* **1987**, *20*, 2740.
(23) Chien, J. C. W.; Hu, Y. *J. Polym. Sci., Part A: Polym. Chem.* **1989**, *27*, 897.
(24) Stukalov, D. V.; Zakharov, V. A.; Potapov, A. G.; Bukatov, G. D. *J. Catal.* **2009**, *266*, 39.
(25) Zakharov, V. A.; Bukatov, G. D.; Barabanov, A. A. *Macromol. Symp.* **2004**, *213*, 19.
(26) Busico, V.; Corradini, P.; Martino, L.; Proto, A.; Savino, V. *Makromol. Chem.* **1985**, *186*, 1279.
(27) Partin, D. E.; O'Keeffe, M. *J. Solid State Chem.* **1991**, *95*, 176.
(28) Perdew, J. P.; Chevary, J. A.; Vosko, S. H.; Jackson, K. A.; Pederson, M. R.; Fiolhais, C. *Phys. Rev. B* **1992**, *46*, 6671.
(29) Vanderbilt, D. *Phys. Rev. B* **1990**, *41*, 7892.
(30) Baroni, S.; Dal Corso, A.; de Gironcoli, S.; Giannozzi, P.; Cavazzoni, P.; Balladio, G.; Scandolo, S.; Chiarotti, G.; Focker, P.; Pasquarello, A.; Laasonen, K.; Trave, A.; Car, R.; Marzari, N.; Kokalj, A. www.pwscf.org/.
(31) Mattsson, A. E.; Armiento, R.; Schultz, P. A.; Mattsson, T. R. *Phys. Rev. B* **2006**, *73*, 195123.